

Electrochemical Biosensor for Sensitive Detection of Hepatitis B in Human Plasma

Ana Graci Brito-Madurro (✉ agbrito@iqufu.ufu.br)

Unievrsidade Federal de Uberlandia

Ana Cristina Honorato Castro

Federal University of Uberlandia: Universidade Federal de Uberlandia

Leandro Toshio Kochi

Butantan Institute: Instituto Butantan

José Manuel Rodrigueiro Flauzino

Federal University of Uberlandia: Universidade Federal de Uberlandia

Marcia Maria Costa Nunes Soares

Adolfo Lutz Institute: Instituto Adolfo Lutz

Valéria Almeida Alves

UFTM: Universidade Federal do Triangulo Mineiro

Luiz Antônio Silva

Universidade Federal do Triangulo Mineiro

João Marcos Madurro

Federal University of Uberlandia: Universidade Federal de Uberlandia

Research Article

Keywords: Electrochemical biosensor, poly(4-AMP), genomic DNA, hepatitis B virus

Posted Date: June 29th, 2021

DOI: <https://doi.org/10.21203/rs.3.rs-544015/v1>

License:  This work is licensed under a Creative Commons Attribution 4.0 International License.

[Read Full License](#)

Abstract

In this work we report the construction of an electrochemical device for molecular diagnosis of hepatitis B virus in the blood plasma of infected patients, using graphite electrodes functionalized with poly(4-aminophenol) and sensitized with specific DNA probe. The recognition of genomic DNA was evaluated by electrochemical techniques (DPV and EIS) and scanning electron microscopy. The genosensor was efficient in detecting genomic DNA with a linear range from $1.176 \mu\text{g}\cdot\text{ml}^{-1}$ to $4.825 \mu\text{g}\cdot\text{ml}^{-1}$ and detection limit of $35.69 \text{ ng}\cdot\text{ml}^{-1}$ ($4.63 \text{ UI}\cdot\text{ml}^{-1}$ or $25.93 \text{ copies}\cdot\text{ml}^{-1}$), which is better than $10.00 \text{ UI}\cdot\text{ml}^{-1}$ limit of reference method, real-time PCR, used in point of care. EIS analysis shows that the genosensor resistance increased exponentially with the concentration of the genomic DNA target. The developed platform has inherent advantages to its applicability in real samples, such as good sensitivity, selectivity, and low sample volume, being interesting for application in diagnosis of hepatitis B virus in blood plasma.

1. Introduction

Hepatitis B is a common viral infection, highly infectious and difficult to treat. It is caused by a DNA virus (HBV) causing irritation and inflammation of the liver. It is a major cause of chronic liver disease, cirrhosis and primary liver cancer. It is estimated that about 2 billion people worldwide have been infected with HBV at a time of life, and of this total over 400 million suffer from the chronic form of the disease [1, 2].

The chronic form of hepatitis B is a serious and silent disease, once some patients are asymptomatic during acute phase, but the liver is gradually destroyed. It can progress to hepatocellular carcinoma and liver cirrhosis and poses great risks to human health [3].

The HBV can be found in blood and other body fluids [3]. The methods currently used for diagnosis of hepatitis B are performed through serological tests such as the enzyme-linked immunosorbent assay (ELISA), immunofluorescence and polymerase chain reaction (PCR) [4]. It is important to note that these assays require the use of reagents in high quantity, skilled labor and expensive equipment that prevents the implementation of these methodologies outside the laboratory environment [5].

When the diagnosis is not early, the patient has a serious medical condition and treatment and cure become more difficult [6]. It is reported that 95% of patients with acute hepatitis B who had early diagnosis showed a good recovery [7]. On the other hand, monitoring should be constant in the chronic phase of the disease to prevent progression of the disease and prevent death. Therefore, it is of the utmost importance diagnostic methods be rapid, highly sensitive and selective, and make it possible to detect and/or monitor the disease in real time, while at the same time being accessible to the entire population [7, 8].

Thus, the electrochemical biosensor technologies have such advantages as fast procedure, low cost, high sensitivity and selectivity and are suitable for diagnostic use [9]. These can be modified with

nanotechnological materials, such as polymeric films [10], carbon nanotubes [11], quantum dots [12], metallic nanoparticles (gold, platinum, palladium and other metals) [13-16].

Electrochemical genosensors are constructed using surface immobilized DNA sequences, functioning as a biological recognition element of the complementary sequence present in the sample to be analyzed, and hybridization can be monitored and analyzed with high sensitivity, from a small amount of sample and reduced dimensions of the working electrode, which can be manufactured at a low cost [17, 18].

The preparation of polymers by electrochemical methods is relatively simple and highly reproducible [19]. There is a great variety of materials that can be used in the construction of polymer films, being fundamental that they allow the immobilization of active species, increase the transfer of electrons and improve the selectivity through the blocking of interferents [10]. Several electrochemical biosensors that use the genetic material for the detection of diseases can be found in the literature, for example for meningococcal meningitis [20], Epstein-Barr virus [21], the oncogenic marker MYCN [22], hepatitis C virus [23, 24], Zika virus [25] and *Mycobacterium leprae* [26]. Srisomwat and collaborators [3] described a device based on 3D microfluidic paper (μ PAD) for detecting HBV DNA. This sensor detected HBV DNA using hexacyanoferrate (III) / (II) as an electrochemical indicator and a linear range of 50 pM-100 nM was obtained with a detection limit of 1.45 pM. Zhao and collaborators [27] built an electrochemical sensor for the analysis of HBV DNA. For this, they used nanoflowers, gold nanoparticles and two aptamers immobilized on the surface to amplify the signal. They obtained a detection limit of 1100 copies. ml⁻¹ and a linear range from 1.10×10^3 to 1.21×10^5 copies.ml⁻¹.

In this work, we build DNA biosensor based on a graphite electrode coated with poly(4-AMP) and functionalized with a specific oligonucleotide probe to detect HBV. The representative scheme is demonstrated below (Figura 1). The viral DNA detection was performed indirectly by monitoring the oxidation peaks the ethidium bromide (EB) intercalator using electrochemical techniques. Furthermore, confirmed with surface scanning electron microscopy (SEM) and successfully tested in patient plasma samples.

2. Experimental

2.1 Materials

All reagents used were of analytical grade without previous purification. Ultra-high purity water (Millipore Milli-Q system, Burlington, USA) was used for the preparation of all the solutions.

The monomer 4-aminophenol (4-AMP) was purchased from Acros Organics (Belgium) HClO₄ (70%) were obtained from Sigma-Aldrich (San Luis, USA) and ethidium bromide (3,8-diamino-5-ethyl-6-phenyl phenatridinium bromide) purchased from Merck KGaA (Darmstadt, Germany). For detection studies, phosphate buffer 0.1 mol L⁻¹ (Na₂HPO₄ 0.061 mol L⁻¹, NaH₂PO₄ 0.039 mol L⁻¹ at pH value 7.3) and the

5.00 mmol L⁻¹ K₄Fe(CN)₆/K₃Fe(CN)₆ containing 0.10 mol L⁻¹ KCl solution was prepared. All solutions were previously deoxygenated by bubbling N₂ before utilization.

Stock solutions of DNA probe and target were prepared in SSC buffer (sodium chloride 0.3 mol L⁻¹, sodium citrate 0.03 mol L⁻¹; Sigma-Aldrich) at pH 7.0 and storage at -12 °C. Specific oligonucleotides for HBV were selected based on conserved aligned regions and synthesized by Alpha DNA (Montreal, Canada). DNA fragments have the related sequences: DNA probe (Hep1): 5'-GAGGAGTTGGGGGAGCACATT-3'; DNA target (Hep2): 5'-AATGTGCTCCCCCAACTCCTC-3'.

The samples of purified viral genomic DNA (DNAGen positive and DNAGen negative), blood plasma from hepatitis B negative (plasma DNA negative) or positive patients (plasma DNA positive) were used for the detection. The genomic DNA was extracted automatically by ABBOTT's m2000sp extractor and the sample concentrations were determined considering the viral load by the PROMEGA Corporation ABBOTT mSample Preparation System DNA kit, obtaining the following concentrations: A1: 436 UI ml⁻¹; A2: 14697 UI ml⁻¹; A3: 24480 UI ml⁻¹; A4: 38000 UI ml⁻¹; A5: 81550 UI ml⁻¹; A6: 100000 UI ml⁻¹. The genomic DNA samples were diluted in SSC buffer and quantified in the Biodrop Duo UV-Vis Spectrophotometer (BioDrop) obtaining the following concentrations: A1: 1.18 µg.ml⁻¹ (4.36 UI.ml⁻¹); A2: 2.17 µg.ml⁻¹ (146.97 UI.ml⁻¹); A3: 3.27 µg.ml⁻¹ (244.80 UI.ml⁻¹); A4: 3.95 µg.ml⁻¹ (380.00 UI.ml⁻¹); A5: 4.21 µg.ml⁻¹ (407.75 UI.ml⁻¹); A6: 4.82 µg.ml⁻¹ (500.00 UI.ml⁻¹).

2.2 Apparatus

Abbott m2000sp extractor (Abbott Laboratories, Chicago, USA) was used to the extraction of genomic DNA. The electrochemical studies were performed in a potentiostat from CH Instruments model 760C (CH Instruments, Austin, USA) using three-compartment and one-compartment cells for eletrodeposition and detection of biomolecules, respectively. A graphite disk, 6 mm diameter, was used as working electrode. Platinum plate and silver/silver chloride (Ag/AgCl, KCl 3.0 mol L⁻¹) electrodes were used as counter electrode and reference electrode, respectively. Electrochemical impedance spectroscopy was performed in an Autolab Electrochemical System (PGSTAT302 N and NOVA 1.10; Metrohm, Herisau, Switzerland). The morphology of the surface of the graphite electrode, the polymeric film, in the absence or in presence of biomolecules and plasma was evaluated using Scanning electron microscopy.

2.3 Functionalization of graphite surface

A solution of 4-AMP (2.5 mmol.L⁻¹) was deaerated with ultra-pure nitrogen for 45 minutes. The electropolymerization of the monomer on the surface of the graphite electrode was performed according to literature [20]. Then, the modified electrode was rinsed with deionized water to remove unreacted monomers.

2.4 HEPB1 probe immobilization on modified graphite electrode and hybridization detection

For the probe immobilization, 18 μL of Hep1 ($63 \mu\text{mol.L}^{-1}$) was dripped onto the modified electrodes and dried at room temperature ($25 \pm 1 \text{ }^\circ\text{C}$) for 5, 10, 20 and 30 minutes. The electrode was immersed for 6 s in phosphate buffer under agitation to remove biomolecules which have not been adsorbed, and then maintained in a solution of 0.5% w/v BSA (bovine serum albumin) by 1 h at $37 \text{ }^\circ\text{C}$. After this step, the electrode was washed in phosphate buffer and dried with ultra-pure nitrogen.

The complementary target detection (Hep2) was performed indirectly by monitoring the oxidation peaks of EB, which amplifies the response signal. For detection, 18 μL of Hep2 solution ($189 \mu\text{mol.L}^{-1}$) was dripped onto the modified electrode and maintained at $55 \text{ }^\circ\text{C}$ for 5, 10, 20 and 30 minutes to promote hybridization. The hybridization temperature was calculated using Gene Runner v3.05 software. Thereafter, the electrode was rinsed in phosphate buffer and 18 μL of EB solution ($1 \mu\text{mol.L}^{-1}$) was added and maintained for 5 minutes at room temperature, followed by the same washing and drying procedure. For statistical analysis, the EB oxidation peak was compared between the different incubation times by Student's t-test and values below 0.05 was considered statistically significant. However, there was no statistically significant difference between the minimum and maximum incubation times. Therefore, the time of 10 minutes was used as a standard for subsequent tests to ensure the probe-target hybridization.

2.5 Calibration curve

The calibration curve was constructed based on the analysis of the oxidation voltammograms of ethidium bromide. The concentration of the Hep1 probe ($63 \mu\text{mol.L}^{-1}$ in SSC buffer) was maintained and varying the concentrations of the complementary target / genomic DNA: $1.18 \mu\text{g.ml}^{-1}$ (4.36 UI.ml^{-1}); $2.17 \mu\text{g.ml}^{-1}$ ($146.97 \text{ UI.ml}^{-1}$); $3.27 \mu\text{g.ml}^{-1}$ ($244.80 \text{ UI.ml}^{-1}$); $3.95 \mu\text{g.ml}^{-1}$ ($380.00 \text{ UI.ml}^{-1}$); $4.21 \mu\text{g.ml}^{-1}$ ($407.75 \text{ UI.ml}^{-1}$); $4.82 \mu\text{g.ml}^{-1}$ ($500.00 \text{ UI.ml}^{-1}$). For the statistical analysis, each concentration was averaged and standard deviation based on the experimental triplicate.

2.6 Selectivity study using blood plasma

Plasma from six patients infected with HBV (plasma DNA positive) and one healthy patients (plasma DNA negative) were used for testing with the genosensor. After extracting the genomic DNA, the samples were diluted 1:100 (v/v) or 1:200 (v/v) in SSC buffer maintaining the concentrations used for the construction of the analytical curve. Genomic DNAs extracted from plasma patients were subjected to a denaturing step prior to the hybridization process.

The solutions were prepared incubated at $98 \text{ }^\circ\text{C}$ for 3 minutes. To avoid double-strand renaturation and to allow complementary and non-complementary DNAs to access the probe in the same condition, the modified electrodes, poly (4-AMP/Hep1) were also incubated at same temperature. Immediately thereafter, 18 μL of the genomic DNA solutions were dripped into the modified electrodes. They were then oven dried for 10 minutes at $55 \text{ }^\circ\text{C}$ to promote hybridization. After this process, washing with phosphate buffer was carried out for the removal of the unbound molecules.

The detection of genomic DNA was performed indirectly using the EB mediator, which amplifies the response signal. To this end, 18 μl of a solution of EB ($1 \mu\text{mol.L}^{-1}$) was added to the electrodes for 5 minutes at room temperature, followed by washing with the phosphate buffer solution. All experiments were performed in triplicate.

2.7 Electrochemical impedance spectroscopy (EIS)

The fundamental steps for the construction of the genosensor were accompanied by the electrochemical impedance spectroscopy technique. The measurements of the EIS was performed at perturbation amplitude of 10 mV and frequency range of 10 kHz to 0.1 Hz in $5.00 \text{ mmol.L}^{-1} \text{ K}_4\text{Fe(CN)}_6/\text{K}_3\text{Fe(CN)}_6$ containing $0.10 \text{ mol.L}^{-1} \text{ KCl}$. All experiments were performed in triplicate.

3. Results And Discussion

3.1 Immobilization and oligonucleotide hybridization

The sensitivity of the DPV technique is appropriate for the electrochemical characterization of the genosensors. Thus, different conditions of immobilization time of the probe (Hep1) and the hybridization time with the complementary target (Hep2) were verified in order to maximize biological recognition and potentially increase the sensitivity of the genosensor (Figure 2).

In FIGURE 2 (A) a study on the immobilization of the Hep1 probe is presented, considering the direct detection of the immobilized biological material. For this, the peak at +0.98 V was taken into account, which can be attributed to the oxidation process of guanine, present in the probe [2]. The intensity of this oxidation peak is proportional to the amount of guanine immobilized on the electrode surface and, providing immobilization of Hep1. We can observe in the time of 30 minutes, a maximum increase was obtained at the peak of the guanine oxidation current, which was two times bigger in relation to the initial immobilization of 5 min. The current values obtained from the guanine oxidation peak remained stable after 30 minutes, indicating that it has the maximum optimum time for coating the electrode with Hep1 in these conditions.

Ethidium bromide (EB) is an efficient electroactive intercalator to the DNA hybridization, due to the oxidation peak around +0.65 V [20, 21], where the peak current intensity is proportional to the accumulation of genetic material on the electrode surface. This response occurs by the intercalation of BE with double-stranded DNA, which is considered the result of the interaction of a hydrophobic aromatic molecule with the hydrophobic environment of the DNA nitrogenous base pairs [28].

Figure 2 B illustrates the assay in which EB was tested on the bioelectrode for the indirect detection of the target Hep2 oligonucleotide. The average value of the oxidation intensity of the experimental control, that is, the bioelectrode containing only the Hep1 probe (0 min) was around 8 μA . An increase in the oxidation intensity of EB is observed with the increase in the time of Hep2 hybridization with the bioelectrode probe, obtaining a maximum value after 30 minutes of incubation. This difference is statistical and we can

consider that EB was retained on the surface due to the presence of the hybridized product. However, between the studied times there were no considerable differences. Therefore, the time used in the next experiments was 5 min. sufficient time to guarantee the best result in the exposure time of the DNA hybridized with EB.

3.2 Calibration curve

The genosensor calibration was conducted varying the concentration of HBV genomic DNA and monitoring the oxidation peak of EB using differential pulse voltammetry (Figure 3). Sensitivity is considered an important property of a biosensor that allow the target analyte detection in minimal concentrations, favoring an early monitoring and detection.

As evident from the voltammograms indicated in Fig. 3A, the response signal of EB increase with the genomic DNA target concentration. The increase in the in the oxidation current response of EB with target concentration occurs due to the pairing process that forms the duplex DNA, which allows the intercalation of increasing quantities of ethidium bromide. Ethidium bromide binds to DNA by intercalation, that is insertion between the stacked base pairs of the double helix [29].

According to Figure 3A, an increase in resistance with increase in the formation of double stranded DNA caused by accumulation of the ethidium bromide onto surface and displacement of the EB oxidation peak to anodic potential more, reinforcing that the hybridization reaction occurs on the surface of the modified electrode.

The behavior of the calibration curve demonstrated that the interleaving speed of ethidium bromide increases linearly in relation to the number of hybrids formed. The genosensor reached a detection limit of 35.69 ng.ml^{-1} (4.63 UI.ml^{-1}) and a quantification limit of $118.90 \text{ ng.ml}^{-1}$ (15.42 UI.ml^{-1}). The linearity (r) between the load and the DNA concentration is 0.999 and the sensitivity is $3.502 \times 10^{-5} \mu\text{g.ml}^{-1} / \mu\text{C}$ or $2.700 \times 10^{-7} \text{ UI.ml}^{-1} / \mu\text{C}$. These values can also be expressed by copies.ml^{-1} for this it is necessary to use a conversion factor, where 1 UI.ml^{-1} is equivalent to $5.6 \text{ copies.ml}^{-1}$ [30, 31]. Therefore, we can still define the detection limit and quantification limit values, respectively, $25.93 \text{ copies.ml}^{-1}$ and $86.35 \text{ copies.ml}^{-1}$. Demonstrating to be more sensitive than the techniques explored in the literature [27].

Traditional methods of molecular analysis of the hepatitis B virus occur through real-time PCR assays, whose average detection limit is 10 UI.ml^{-1} [32-34]. This technique for diagnosis is expensive, once requires qualified labor and takes a long time, facts that hinder its point-of-care applicaton. Thus, this new genosensor presents attractive features for the application in diagnostics due to the higher sensitivity, quickness and lower manufacturing cost.

3.3. Electrochemical Impedance Spectroscopy of the genosensor platform

Electrochemical impedance spectroscopy (EIS) studies is a powerful and sensitive tool for studying the charge transfer processes occurring at the electrode-solution or modified electrode-solution interfaces

[35]. The EIS technique was used to verify the immobilization of the DNA probe on a surface of the poly(4-AMP)-modified graphite electrode, as well the subsequent hybridization with the complementary genomic DNA. Figure 4 shows the Nyquist plots of the EIS data of the modified electrode before and after the DNA probe immobilization, as well with the different concentrations of the target DNA (DNAgen). In addition to the electrical parameters obtained through an equivalent electrical circuit.

Analyzing the behavior at high frequencies (Fig 4A), it is possible to see the formation of a semicircle in the complex plane with the addition of the Hep1 DNA probe. The immobilization of the Hep1 probe on the surface of the modified graphite electrode creates a thin film which hamper the electron transfer from the redox pair ferro/ferricyanide to the electrode, increasing the charge transfer resistance of the system. In Fig. 3B the behavior of the impedance spectra at high frequencies shows great coherence with the expected, which is a process of hybridization of the DNA single strand Hep1 probe with the DNAgen. The increase in the resistivity of the genosensor with the increase in the concentration of the DNAgen was related to the intercalation of DNAgen inside the probe and, in the sequence, a probable combination between the nitrogenous bases to form the double helix of DNA. This layer of DNA double helix formed on the electrode makes it less porous, behaving like a passive film, making the passage of electric current difficult.

The equivalent circuit shown in Figure 4 C and D was chosen because it presents more coherent and reproducible results for the genosensor. The results obtained with the simulation for each DNAgen concentration are consistent with their intercalation and, consequently, hybridization with Hep1. The effects of hybridization are observed in the exponential increase in the resistance of the hybridized film and in the charge transfer resistance of the Fe^{2+}/Fe^{3+} system, and in the decrease in the capacitance of the hybridized film and the capacitance of the double layer of the genosensor.

Analyzing the results of the modified electrode with the hybridized film that appears at high frequencies, it was observed that the R_f increased exponentially with the increase in the concentration of the genomic DNA target (DNAgen). The increase in R_f is related to the higher compacting of the hybridized film, increasing the coverage of the geometric area of the graphite electrode. This phenomenon is related to equation (1):

$$R_f = \rho \frac{l_{film}}{A_{substrate}}$$

where, ρ is the resistivity of the hybridized film, l_{film} is the thickness of the hybridized film and $A_{substrate}$ is the uncovered area of the graphite electrode modified with poly(4-AMP). The opposite effect was observed for the film capacitance, Q_f , being consistent with equation (2):

$$Q_f = \epsilon \epsilon_0 \frac{A_{substrate}}{l_{film}}$$

where, ϵ denotes the dielectric constant relative to the DNA probe (Hep1) and the hybrid formed with the complementary target of genomic DNA (positive DNAGen) and ϵ_0 is the permittiveness of the vacuum ($8.85 \cdot 10^{-14} \text{ F cm}^{-1}$).

The Q_f values are related to the decrease in the dielectric constant, because of the elimination of porosity in the film, causing a reduction of the exposed geometric area of the graphite electrode and greater thickness of the hybridized film. The interpretation of the electrical behavior of the components R_f and Q_f is closely related to the time constant at low frequencies, described by the electrical components R_{ct} and Q_{dl} . The decrease in Q_{dl} with simultaneous increase in R_{ct} indicates that there was complete coverage of the graphite electrode with the poly(4-AMP) substrate, the effective adsorption of the Hep1 and the greater hybridization with the increase in the concentration of the DNAGen.

3.4 Specificity using genomic DNA in real samples and microscopy analysis

The detection of the target analyte in patient samples is an extremely important step to verify the accuracy of the diagnosis [36]. It is known that human plasma is a fluidic mixture composed of several components that can interfere with the reading of the signal, and therefore, it is necessary to evaluate the device's ability to distinguish the target molecule from the contaminants to have a more accurate diagnosis [37]. Figure 5 (A) shows the specificity study of the system in which the sensor was tested in the presence (positive Plasma – control positive) and in the absence (healthy plasma – control negative) of the genetic material. The applicability of the sensor was evaluated using sample of 5 patients, comparing the obtained results in the presence and absence of blood plasma. For this analysis, the plasma samples were diluted, maintaining the same concentrations of the genomic DNA, in SSC buffer, shown in Figure 5 (B).

Fig 5A shows the comparison of the electrochemical signal before the formation of the duplex (curve a), and in the presence of DNAGen (curve c), positive plasma (curve d) and plasma negative (curve b). In the presence of the target DNAGen (curve c), there was an increase in the electrochemical response of EB, indicating that the molecular recognition occurred efficiently, since the signal is proportional to the concentration of interlayer fixed on the surface [5]. In addition, we can observe that there was a displacement of the potential for anodic regions, from +0.69V to +0.74 V, showing an increase in resistance to charge transfer, thus confirming the formation of the duplex (Hep1: DNAGen) in agreement with electrochemical impedance spectroscopy data. This same shift is also seen in figure 3A, reinforcing the idea of genetic molecular recognition.

When working with blood plasma samples (Fig 5A – curves a and d), we can also observe a shift in the oxidation potential of EB to anode potentials. With the complexity that plasma samples represent to electronic systems, we can suggest that the shift, and consequently the increase in resistance, are related to some non-specific interactions that may occur between the complex sample and the platform. We can still believe that due to the size of the genetic molecule it is possible to form hairpin loop structures, where two regions of the same molecule can interact and increasing resistance [38, 39].

Another observed fact is the increase in the oxidation intensity of EB. The addition of negative plasma (Fig 5 A - curve b) does not considerably influence the oxidation potential and the response of the electrical indicator (EB). Even so, it promotes a small increase in current, this may be related to the constituents present in the plasma sample that interacted not specifically with the Hep1 probe and, consequently, a small amount of EB can be captured and oxidized, however this accumulation does not impair the response of the genosensor to the presence of viral genetic material. As in the negative sample, it promoted an insignificant increase in the electrochemical signal, strengthening the proposal that the presence of plasma does not influence the final response, suggesting that the platform is an excellent option for real-time diagnosis.

In the presence of positive plasma (Figure 5 A - curve d), an intense peak of EB oxidation is observed, indicating that the Hep1 probe was efficient in recognizing and promoting hybridization with the complementary region of the genomic DNA present in the sample, allowing the connection of EB in the duplex formation. When comparing Fig. 5 A – curve c in relation to the Fig. 5 A - curve d, we can see that the current values obtained are similar, however the positive plasma sample shows a slight increase in intensity and a slightly more pronounced displacement when compared to the probe, + 0.69 V to +0.76 V, due to possible non-specific interactions [20]. This behavior is followed for samples from 5 sick patients and shown in Fig. 5 B. We observed the same behavior for all samples. Secondary genetic structures and non-specific interactions can act as anchors and retain some EB on the surface. With a washing of the surface and the thermal process by which the sample was submitted, these interactions are minimized to the point of not causing significant interference in the electrochemical analysis. Therefore, only the genetic material of the virus would be retained on the surface.

The system is able to distinguish the concentration of genomic DNA, in the absence and presence of blood plasma, and the biosensor response is not significantly affected in the presence of plasma, showing a promising device for the diagnosis of hepatitis B.

Analysis by scanning electron microscopy were carried out modified graphite electrodes (Figure 5 A - images a-d). The images suggest that the modification was carried out successfully, and that they have very different characteristics between them. Highlighting indicated in the Figure 5A – image d, which in the presence of plasma caused the most significant change, was presenting some globular structures.

4. Conclusion

The agreement of the results obtained with the different techniques utilized points to a promising application of the DNA genosensor developed for the point of care. It was observed agreement between the results obtained using differential pulse voltammetry, electrochemical impedance and scanning electron microscopy.

The high reproducibility for the target recognition and duplex formation (hepB1:hepB2) using ethidium bromide giving credibility to the diagnosis.

The genosensor was efficient in detecting genomic DNA with high sensitivity, a low wide dynamic detection range, detection limit better than a reference method used, and could effectively discriminate complementary target sequence without the need for prior purification of the sample.

The genosensor has advantages over serological techniques, such as miniaturization, low cost, *in situ* analysis in real time, allowing evaluating the viral load present in the patient.

Declarations

Ethical Approval

All studies were approved by a Research Ethics Committee (EC: 1.131.34).

Consent to Participate

All authors agree to participate of this work.

Consent to Publish

All authors consent to publish of the Work.

Authors' contributions

Ana C. H. Castro: Conceptualization, Methodology, Formal Analysis, Investigation, Writing. **Leandro T. Kochi:** Methodology, Investigation, Conceptualization, Writing. **José M. R. Flauzino:** Methodology, Investigation. **Márcia M. C. N. Soares:** Human serum sample supply, methodology. **Valéria A. Alves:** Methodology, Formal Analysis. **Luís A. da Silva:** Methodology, Formal Analysis. **José M. R. Flauzino:** Methodology, Validation, Formal Analysis repetido. **João M. Madurro:** Investigation, Conceptualization, Supervision, Writing - Reviewing and Editing, Funding acquisition. **Ana G. Brito Madurro:** Investigation, Conceptualization, Supervision, Writing- Reviewing and Editing, Funding acquisition.

Funding

All research grants and scholarships were financed by **Coordenação de Aperfeiçoamento de Pessoal de Nível Superior** (CAPES). Scholarships Number: 438316/2018-5, Recipient: Ana Cristina Honarato Castro, Dr and **Conselho Nacional de Desenvolvimento Científico e Tecnológico** (CNPq), Award Number: 310782/20, Recipient: Ana Graci Brito Madurro, PhD.

Competing Interests

There are no competing interest to declare.

Availability of data and materials

Not applicable

References

1. Li XH, Zhang XL, Wu J, Lin N, Sun WM, Chen M, Ou QS, Lin ZY (2019) Hyperbranched rolling circle amplification (HRCAs)-based fluorescence biosensor for ultrasensitive and specific detection of single-nucleotide polymorphism genotyping associated with the therapy of chronic hepatitis B virus infection. *Talanta*. 191:277-82. doi: <https://doi.org/10.1016/j.talanta.2018.08.064>.
2. Castro ACH, França EG, de Paula LF, Soares MMCN, Goulart LR, Madurro JM, Brito-Madurro AG (2014) Preparation of genosensor for detection of specific DNA sequence of the hepatitis B virus. *Appl Surf Sci* 314:273-9. doi: <https://doi.org/10.1016/j.apsusc.2014.06.084>.
3. Srisomwat C, Teengam P, Chuaypen N, Tangkijvanich P, Vilaivan T, Chailapakul O (2020) Pop-up paper electrochemical device for label-free hepatitis B virus DNA detection. *Sens Actuators B Chem* 316:128077. doi: <https://doi.org/10.1016/j.snb.2020.128077>.
4. Yang L, Du F, Chen G, Yasmeeen A, Tang Z (2014) A novel colorimetric PCR-based biosensor for detection and quantification of hepatitis B virus. *Anal Chim Acta* 840:75-81. doi: <https://doi.org/10.1016/j.aca.2014.05.032>.
5. Oliveira DA, Silva JV, Flauzino JMR, Castro ACH, Moço ACR, Soares MMCN, Madurro JM, Brito-Madurro AG (2018) Application of nanomaterials for the electrical and optical detection of the hepatitis B virus. *Anal Biochem* 549:157-63. doi: <https://doi.org/10.1016/j.ab.2018.03.023>.
6. Xiao G, Zhu F, Wang M, Zhang H, Ye D, Yang J, Jiang L, Liu C, Yan L, Qin R. (2016) Diagnostic accuracy of APRI and FIB-4 for predicting hepatitis B virus-related liver fibrosis accompanied with hepatocellular carcinoma. *Digest Liver Dis* 48(10):1220-6. doi: <https://doi.org/10.1016/j.dld.2016.06.001>.
7. Mao X, Liu S, Yang C, Liu F, Wang K, Chen G (2016) Colorimetric detection of hepatitis B virus (HBV) DNA based on DNA-templated copper nanoclusters. *Anal Chim Acta* 909:101-8. doi: <https://doi.org/10.1016/j.aca.2016.01.009>.
8. Mashhadizadeh MH, Talemi RP (2016) Synergistic effect of magnetite and gold nanoparticles onto the response of a label-free impedimetric hepatitis B virus DNA biosensor. *Mater Sci Eng C* 59:773-81. doi: <https://doi.org/10.1016/j.msec.2015.10.082>.
9. Liu CJ, Williams KE, Orr HT, Akkin T (2017) Visualizing and mapping the cerebellum with serial optical coherence scanner. *Neurophotonics* 4(1):011006-. doi: <https://doi.org/10.1117/1.NPh.4.1.011006>.
10. Rodrigues LP, Ferreira DC, Ferreira LF, Cuadros-Orellana S, de Oliveira GC, Brito-Madurro AG, Madduro JM (2015) Electropolymerization of hydroxyphenylacetic acid isomers and the development of a bioelectrode for the diagnosis of bacterial meningitis. *J Appl Electrochem* 45(12):1277-87. doi: <https://doi.org/10.1007/s10800-015-0892-2>.

11. Jasim A, Ullah MW, Shi Z, Lin X, Yang G (2017) Fabrication of bacterial cellulose/polyaniline/single-walled carbon nanotubes membrane for potential application as biosensor. *Carbohydr Polym* 163:62-9. doi: <https://doi.org/10.1016/j.carbpol.2017.01.056>.
12. Deng H, Li Z, Bian Z, Yang F, Liu S, Fan Z, Wang Y, Tang G (2017) Influence of measurement uncertainty on the world health organization recommended regulation for mainstream cigarette smoke constituents. *Regul Toxicol Pharmacol* 86:231-40. doi: <https://doi.org/10.1016/j.yrtph.2017.03.010>.
13. Lu Q, Wang H, Liu Y, Hou Y, Li H, Zhang Y (2017) Graphitic carbon nitride nanodots: As reductant for the synthesis of silver nanoparticles and its biothiols biosensing application. *Biosens Bioelectron* 89:411-6. doi: <https://doi.org/10.1016/j.bios.2016.05.064>.
14. Presnova G, Presnov D, Krupenin V, Grigorenko V, Trifonov A, Andreeva I, Ignatenko O, Egorov A, Rubtsova M (2017) Biosensor based on a silicon nanowire field-effect transistor functionalized by gold nanoparticles for the highly sensitive determination of prostate specific antigen. *Biosens Bioelectron* 88:283-9. doi: <https://doi.org/10.1016/j.bios.2016.08.054>.
15. Rezaei B, Shams-Ghahfarokhi L, Havakeshian E, Ensafi AA (2016) An electrochemical biosensor based on nanoporous stainless steel modified by gold and palladium nanoparticles for simultaneous determination of levodopa and uric acid. *Talanta* 158:42-50. doi: <https://doi.org/10.1016/j.talanta.2016.04.061>.
16. Skotadis E, Voutyras K, Chatzipetrou M, Tsekenis G, Patsiouras L, Madianos L, Chatzandroulis S, Zergioti I, Tsoukalas D (2016) Label-free DNA biosensor based on resistance change of platinum nanoparticles assemblies. *Biosens Bioelectron* 81:388-94. doi: <https://doi.org/10.1016/j.bios.2016.03.028>.
17. Heli H, Sattarahmady N, Hatam GR, Reisi F, Vais RD (2016) An electrochemical genosensor for *Leishmania major* detection based on dual effect of immobilization and electrocatalysis of cobalt-zinc ferrite quantum dots. *Talanta* 156-157:172-9. doi: <https://doi.org/10.1016/j.talanta.2016.04.065>.
18. Rahi A, Sattarahmady N, Heli H (2016) An ultrasensitive electrochemical genosensor for *Brucella* based on palladium nanoparticles. *Anal Biochem* 510:11-7. doi: <https://doi.org/10.1016/j.ab.2016.07.012>.
19. Castro ACH, Alves LM, Siquieroli ACS, Madurro JM, Brito-Madurro AG (2020) Label-free electrochemical immunosensor for detection of oncomarker CA125 in serum. *Microchem J* 155:104746. doi: <https://doi.org/10.1016/j.microc.2020.104746>.
20. Castro ACH, Kochi LT, Moço ACR, Coimbra RS, Oliveira GC, Cuadros-Orellana S, Madurro JM, Brito-Madurro AG (2018) A new genosensor for meningococcal meningitis diagnosis using biological samples. *J Solid State Electrochem* 22(8):2339-46. doi: <https://doi.org/10.1007/s10008-018-3940-0>.

21. Balvedi RPA, Castro ACH, Madurro JM, Brito-Madurro AG (2014) Detection of a specific biomarker for Epstein-Barr virus using a polymer-based genosensor. *Int J Mol Sci* 15(5):9051-66. doi: <https://doi.org/10.3390/ijms15059051>.
22. Silva TDS, Castro ACH, Rodovalho VR, Madurro JM, Brito-Madurro AGB (2016) Development of electrochemical genosensor for MYCN oncogene detection using rhodamine B as electroactive label. *J Solid State Electrochem* 20(9):2411-8. doi: <https://doi.org/10.1007/s10008-016-3326-0>.
23. Singhal C, Ingle A, Chakraborty D, Pn AK, Pundir CS (2017) Narang J. Impedimetric genosensor for detection of hepatitis C virus (HCV1) DNA using viral probe on methylene blue doped silica nanoparticles. *Int J Biol Macromol* 98:84-93. doi: <https://doi.org/10.1016/j.ijbiomac.2017.01.093>.
24. Oliveira DA, Silva JV, Flauzino JMR, Sousa HS, Castro ACH, Moço ACR, Soares MMCN, Madurro JM, Brito-Madurro AG (2019) Carbon nanomaterial as platform for electrochemical genosensor: A system for the diagnosis of the hepatitis C in real sample. *J Electroanal Chem* 844:6-13. doi: <https://doi.org/10.1016/j.jelechem.2019.04.045>.
25. Moço ACR, Guedes PH, Flauzino JMR, Silva HS, Vieira JG, Castro ACH, Gomes EVR, Tolentino FM, Madurro JM, Brito-Madurro AG (2019) Electrochemical Detection of Zika Virus in Biological Samples: A Step for Diagnosis Point-of-care. *Electroanalysis* 31(8):1580-7. doi: <https://doi.org/10.1002/elan.201900068>
26. Afonso AS, Goulart LR, Goulart IMB, Machado AEH, Madurro JM, Brito-Madurro AG (2010) A promising bioelectrode based on gene of *Mycobacterium leprae* immobilized onto poly(4-aminophenol). *J Appl Polym Sci* 118(5):2921-8. doi: <https://doi.org/10.1002/app.32595>.
27. Zhao F, Bai Y, Cao L, Han G, Fang C, Wei S, Chen Z (2020) New electrochemical DNA sensor based on nanoflowers of $\text{Cu}_3(\text{PO}_4)_2$ -BSA-GO for hepatitis B virus DNA detection. *J Electroanal Chem* 867:114184. doi: <https://doi.org/10.1016/j.jelechem.2020.114184>.
28. Waring MJ (1974) Stabilization of two-standard ribohomopolymer helices and destabilization of a three-stranded helix by ethidium bromide. *Biochem J* 143(2):483-6. doi: <https://doi.org/10.1042/bj1430483>.
29. Pastré D, Piétrement O, Zozime A, Cam E (2005) Study of the DNA/ethidium bromide interactions on mica surface by atomic force microscope: Influence of the surface friction. *Biopolymers* 77(1):53-62. doi: <https://doi.org/10.1002/bip.20185>.
30. European Association For The Study Of The Liver (2012) EASL clinical practice guidelines: Management of chronic hepatitis B virus infection. *J Hepatol* 57(1):167-85. doi: <https://doi.org/10.1016/j.jhep.2012.02.010>.

31. Keefe EB, Dieterich DT, Han SH, Jacobson IM, Martin P, Schiff ER, Tobias H, Wright TL (2006) A treatment algorithm for the management of chronic hepatitis B virus infection in the United States: an update. *Clin Gastroenterol Hepatol* 4(8):936-62. doi: <https://doi.org/10.1016/j.cgh.2006.05.016>.
32. Caliendo AM, Valsamakis A, Bremer JW, Ferreira-Gonzalez A, Granger S, Sabatini L, Tsongalis GJ, Wang YF, Yen-Lieberman B, Young S, Lurain NS (2011) Multilaboratory evaluation of real-time PCR tests for hepatitis B virus DNA quantification. *J Clin Microbiol* 49(8):2854-8. doi: <https://doi.org/10.1128/jcm.00471-11>.
33. Ismail AM, Sivakumar J, Anantharam R, Dayalan S, Samuel P, Fletcher GJ, Gnanamony M, Abraham P (2011) Performance characteristics and comparison of Abbott and artus real-time systems for hepatitis B virus DNA quantification. *J Clin Microbiol* 49(9):3215-21. doi: <https://doi.org/10.1128/jcm.00915-11>.
34. Drexler JF, Reber U, Wuttkopf A, Eis-Hübinger AM, Drosten C (2012) Performance of the novel Qiagen artus QS-RGQ viral load assays compared to that of the Abbott RealTime system with genetically diversified HIV and hepatitis C Virus plasma specimens. *J Clin Microbiol* 50(6):2114-7. doi: <https://doi.org/10.1128/jcm.05874-11>.
35. Han H, Wang C, Ma Z, Su Z (2006) A facile method to produce highly monodispersed nanospheres of cystine aggregates. *Nanotechnology* 17(20):5163-6. doi: <https://doi.org/10.1088/0957-4484/17/20/021>.
36. Riedel T, Surman F, Hageneder S, Pop-Georgievski O, Noehammer C, Hofner M, Brynda E, Rodriguez-Emmenegger C, Dostálek J (2016) Hepatitis B plasmonic biosensor for the analysis of clinical serum samples. *Biosens Bioelectron* 85:272-9. doi: <https://doi.org/10.1016/j.bios.2016.05.014>.
37. Wang X, Li Y, Wang H, Fu Q, Peng J, Wang Y, Du J, Zhou Y, Zhan L (2010) Gold nanorod-based localized surface plasmon resonance biosensor for sensitive detection of hepatitis B virus in buffer, blood serum and plasma. *Biosens Bioelectron* 26(2):404-10. doi: <https://doi.org/10.1016/j.bios.2010.07.121>.
38. Amiri AR, Macgregor RB (2011) The effect of hydrostatic pressure on the thermal stability of DNA hairpins. *Biophys Chem* 156(1):88-95. doi: <https://doi.org/10.1016/j.bpc.2011.02.001>

Tables

Due to technical limitations, table 1 is only available as a download in the Supplemental Files section.

Figures

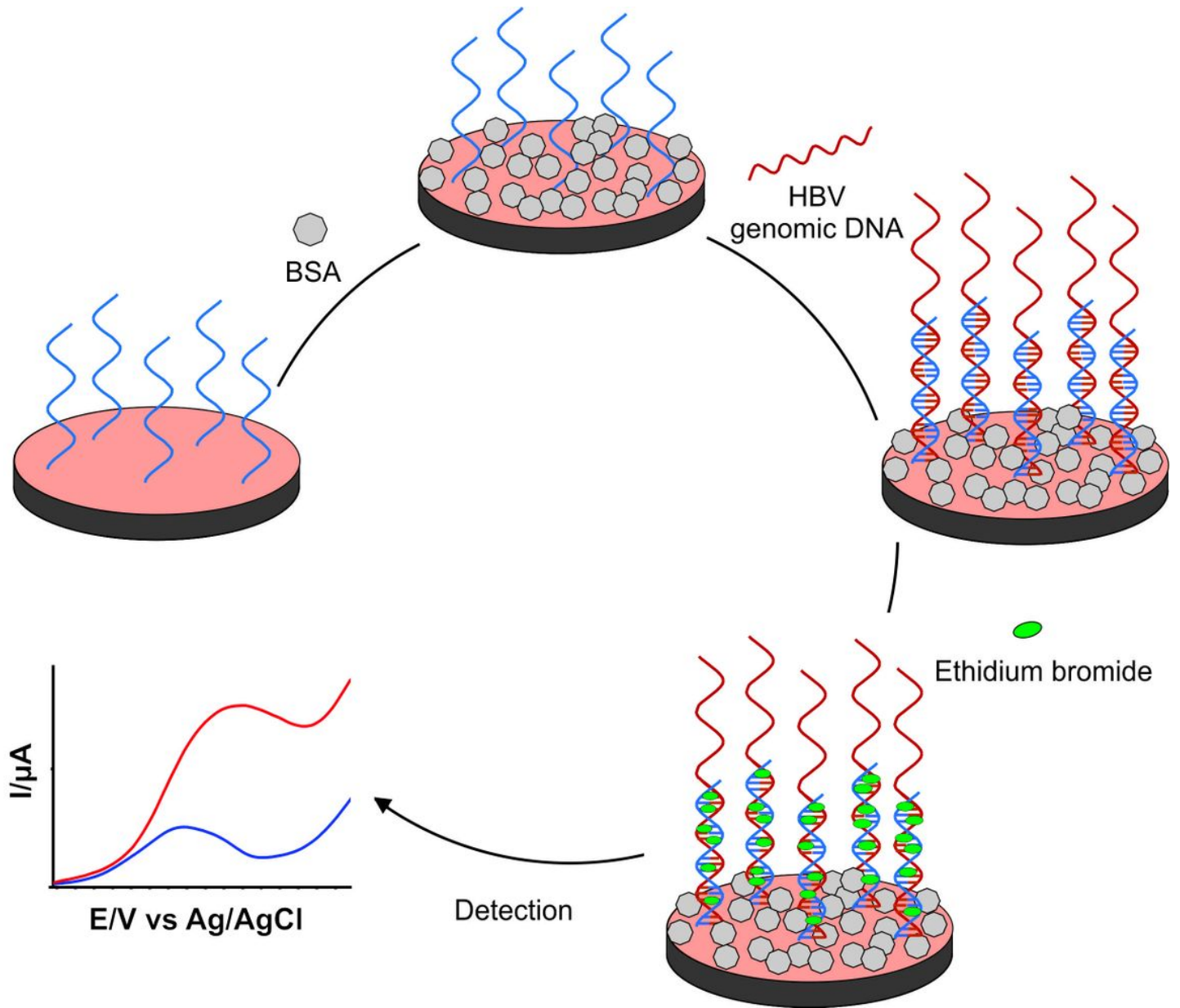


Figure 1

Steps used for the genosensor construction.

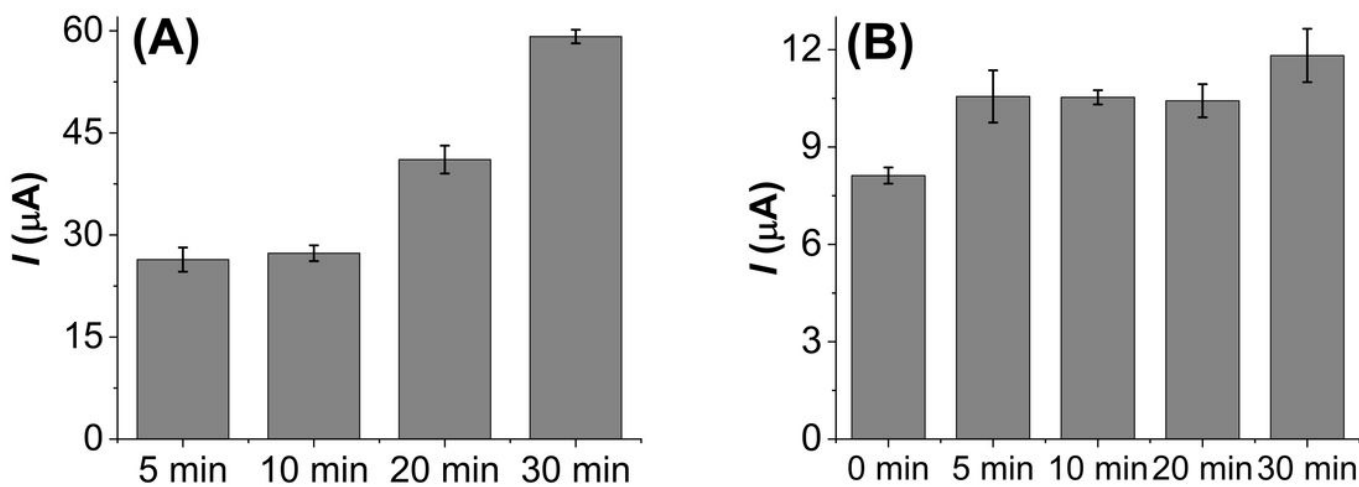


Figure 2

Bar chart of the DPV responses obtained for the modified electrodes. (A) guanine oxidation for the immobilization time of Hep1 probe (A) and ethidium bromide oxidation after hybridization HepB1-Hep2 (B). The illustrated error bars represent the standard deviation across five repetitive experiments (N=3). Electrolyte support: phosphate buffer, pH 7.3, amplitude modulation: 0.05 mV, pulse interval: 0.2 s, scan rate: 20 mV.s⁻¹. Statistical analysis were performed by Student's t-test ($p < 0.05$).

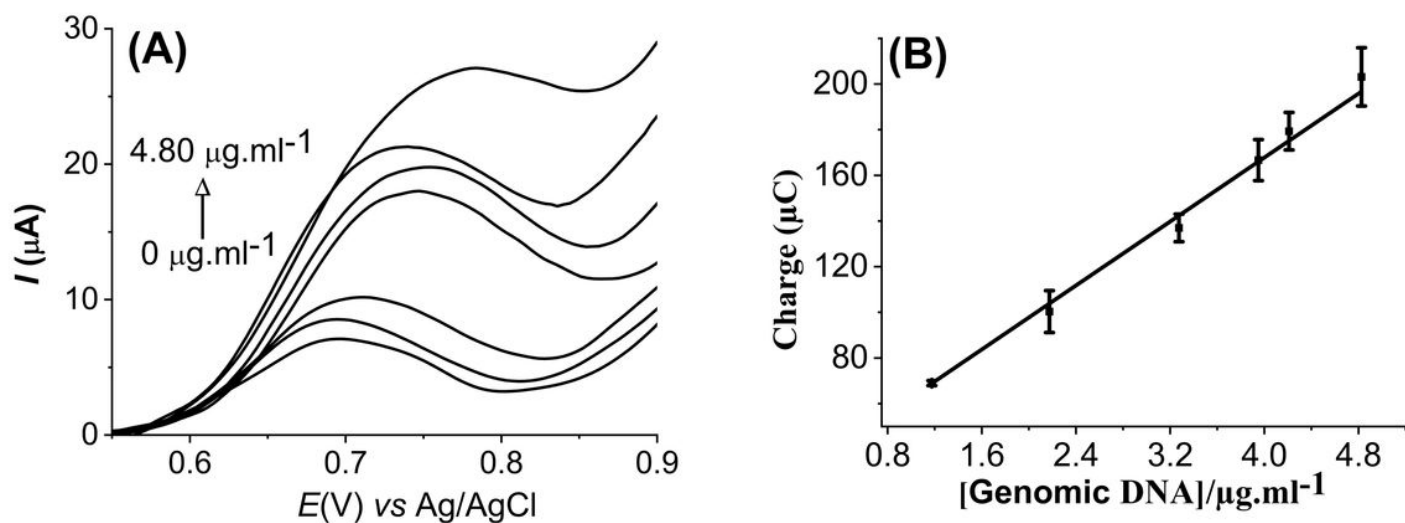


Figure 3

(A) VPD from the oxidation of ethidium bromide on the surface of graphite electrodes functionalized with Hep1-containing poly(4-AMP) before and after hybridization with different concentrations of the genomic DNA target. (B) Calibration curve of genosensor monitoring the ethidium bromide signal of current response versus the genomic DNA concentration (N = 3). Electrolyte: phosphate buffer solution (0.1 mol L⁻¹, pH 7.4). Modulation range: 0.05 mV, pulse interval: 0.2 s, scan rate: 20 mV.s⁻¹.

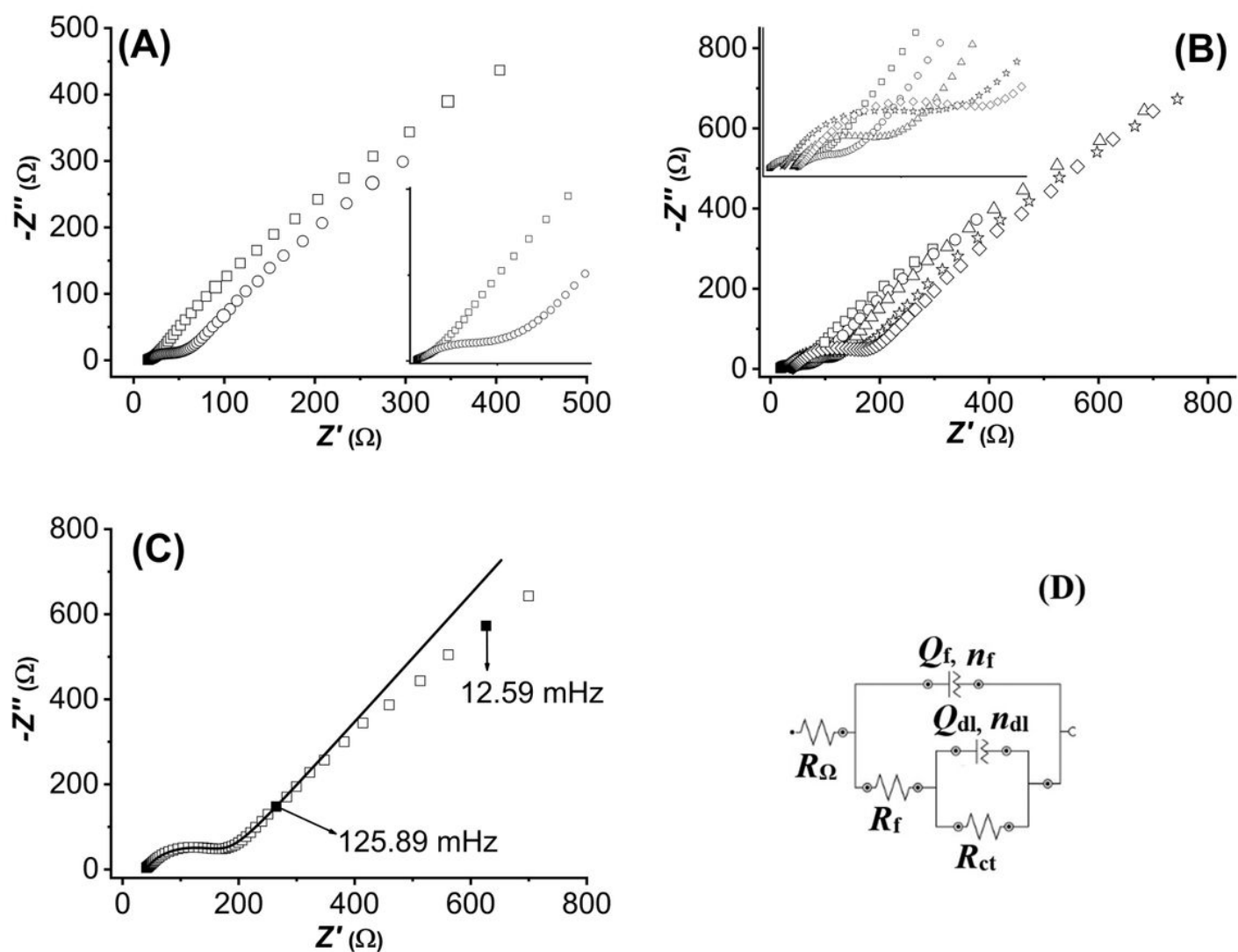


Figure 4

(A) Nyquist plots of the EIS data: (\square) poly(4-AMP); (\circ) Hep1 probe (B) Nyquist plots of the EIS data with different target concentrations: (\square) Hep1 probe; (\bullet) 1.176 de DNAGen; (\triangle) 2.175 de DNAGen; (\boxtimes) 4.210 de DNAGen; (\diamond) 4.825 of DNAGen. Applied potential of +0.23 V in standard solutions of $\text{K}_4[\text{Fe}(\text{CN})_6]$ and $\text{K}_3[\text{Fe}(\text{CN})_6]$ in 5.0 mmol L^{-1} , KCl in 0.1 mol L^{-1} as carrier electrolyte. Insets: The inset on the Nyquist plot indicates a zoom to the high frequency region. (C) Nyquist plots of the EIS data: (\bullet) 4,825 $\mu\text{g L}^{-1}$ of DNAGen; (—) representative simulation of the impedance spectra. Applied potential of +0.23 V in standard solutions of $\text{K}_4[\text{Fe}(\text{CN})_6]$ and $\text{K}_3[\text{Fe}(\text{CN})_6]$ in 5.0 mmol L^{-1} , KCl in 0.1 mol L^{-1} as carrier electrolyte. (D) Equivalent circuit, where R_{Ω} is the ohmic resistance of the electrolyte, Q_f and R_f capacitance and resistance of the Hep1 probe or hybridized Hep1-DNAGen, respectively, R_{ct} is the charge transfer resistance and Q_{dl} is the double layer capacitance.

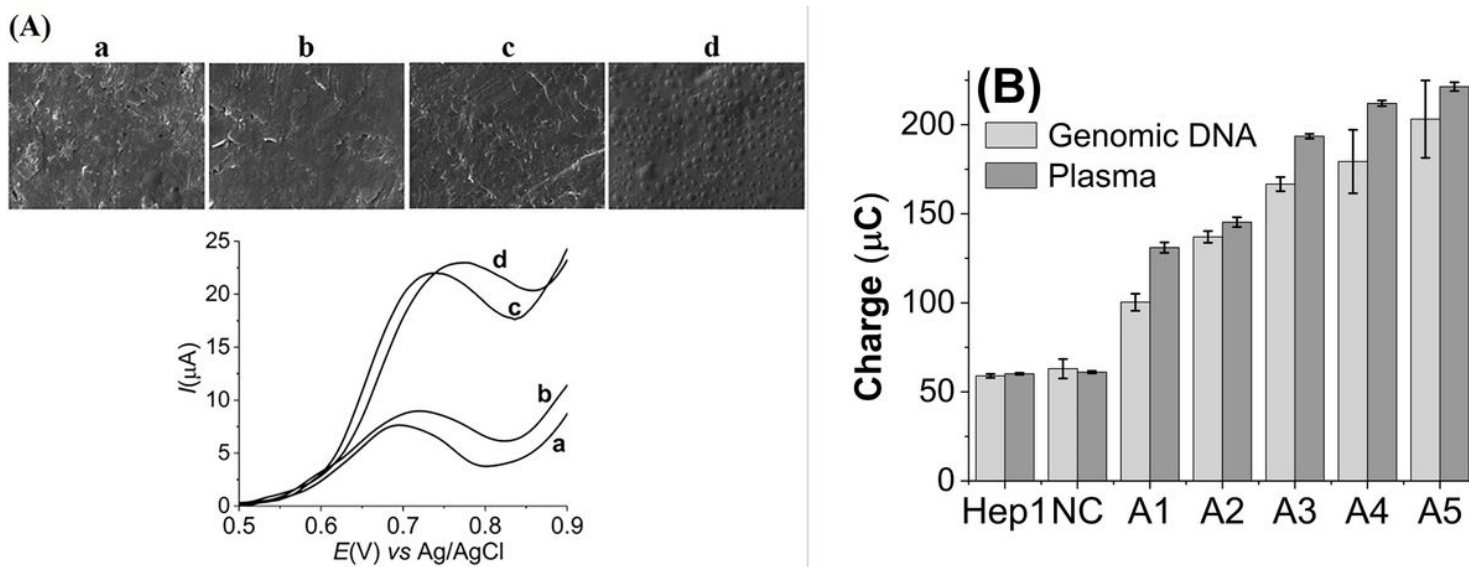


Figure 5

Response of the genosensor using genomic DNA, plasma sample from sick (with HBV) and healthy patients. (A) Scanning electron microscopy (SEM) studies and VPD from the oxidation of ethidium bromide on the surface of graphite electrodes functionalized with Hep1-containing poly(4-AMP)/Hep1 (a); negative plasma (b); after hybridization with genomic DNA (c) and positive plasma (d). (B) Bar chart of current values of the EB oxidation for healthy patient (NC) and sick patients (1 - 5). (A1) 1.176 $\mu\text{g ml}^{-1}$; (A2) 2.175 $\mu\text{g ml}^{-1}$, (A3) 3.275 $\mu\text{g ml}^{-1}$, (A4) 4.210 $\mu\text{g ml}^{-1}$, (A5) 4.825 $\mu\text{g ml}^{-1}$. Electrolyte: 0.10 mol L⁻¹ phosphate buffer, pH 7.4. Modulation amplitude: 25 mV. Pulse interval: 0.2 s; 20 mVs⁻¹ (N = 3).

Supplementary Files

This is a list of supplementary files associated with this preprint. Click to download.

- [Table1.jpg](#)